IEEE Access
Multidisciplinary | Rapid Review | Open Access Journal

Received July 8, 2020, accepted July 14, 2020, date of publication July 17, 2020, date of current version July 29, 2020.

Digital Object Identifier 10.1109/ACCESS.2020.3009972

Multi UAV Cluster Control Method Based on Virtual Core in Improved Artificial Potential Field

ENMING WU, YIDONG SUN, JIANYU HUANG, CHAO ZHANG, AND ZHIHENG LI
Basic Experiment Center, Civil Aviation University of China, Tianjin 300300, China

Corresponding author: Yidong Sun (syd_cauc@outlook.com)

This work was supported by the Fundamental Research Funds for the Central Universities through the Special Project of the Civil Aviation University of China under Grant No. 3122018S007.

ABSTRACT In this paper, a method of multi UAV cluster control based on improved artificial potential field (APF) is proposed. The k-means method is used to integrate and optimize the attractive force between UAVs, and the concept of virtual core is introduced to realize the cluster control and adaptive formation flight of multiple UAVs. The attractive disturbance component of the target point is introduced and the backtracking-filling method is proposed to solve the local minimum problem in the APF. The repulsion force in the APF can realize obstacle avoidance and collision avoidance, and the virtual core can control the UAV cluster to fly to the target point under the attractive force of potential field, so as to realize the track planning and multi aircraft cooperative task. In the process of cluster flight when the UAV fails, merges or dispatches, the method can realize cluster reconfiguration and the cluster control effect and task execution success rate can be improved. The simulation experiments in virtual APF and urban environment APF show the effectiveness of this method.

INDEX TERMS Cluster control, virtual core algorithm, cluster reconstruction, track planning, improved APF.

I. INTRODUCTION

With the rapid development of sensor, cloud computing and communication technology, UAV system is widely used in military and civil fields. However, the task execution ability and efficiency of a single UAV is limited, and the task environment is increasingly complex. Therefore, UAV cluster control technology has been widely studied. The mission process of multiple UAVs includes formation control, track planning, obstacle avoidance of single UAV, collision avoidance of multiple UAVs, collaborative execution and other links.

In order to accomplish multi UAV tasks intelligently and efficiently, the importance of formation control is self-evident. Feasible formation control methods mainly include: leader follower, virtual structure and behavior-based method [1]. Based on the event triggering control strategy of internal and external loop control, the consistency and formation of VTOL UAV cluster are solved [2]. Through the design of the intermediate attitude composed of the desired attitude and position information, an attitude based coupled trajectory tracking scheme is completed to realize the trajectory tracking and formation tracking of the VTOL UAV [3]. Based on the nonsmoothed consistent backstepping design, the master-slave distributed formation control of multiple four rotor aircraft are realized [4]. The leader follower method has the disadvantages of decentralized layout and no feedback information between drones, which leads to the increase of collision probability between drones [5]. In [6], a distributed control architecture is designed based on the dynamic system theory to realize the formation control based on behavior. Based on the demonstration of formation flying performance, the dynamic performance of UAV is reflected through the information sharing system of sensors on the UAV and formation flying algorithm [7]. The above research about formation control algorithm has achieved a good formation configuration, but it cannot guarantee the flexibility in the complex task environment.

When the UAV is performing tasks in unstructured environment, track planning, obstacle avoidance of single UAV

The associate editor coordinating the review of this manuscript and approving it for publication was Gustavo Olague.

This work is licensed under a Creative Commons Attribution 4.0 License. For more information, see https://creativecommons.org/licenses/by/4.0/

and collision avoidance of multiple UAVs are very important issues. Based on the three-dimensional probability road map, multi trajectory planning is carried out for UAV group to deal with urban building emergencies [8]. By introducing additional control force to improve APF, UAV path planning can be effectively and conveniently realized [9]. Particle swarm optimization fuzzy control method [10], [11], artificial potential tangent vector method [12], improved APF method based on case reasoning [13] and other applications in path planning of mobile robots provide experience for UAV path planning. The ellipsoid is used as the restricted area of the obstacle, and the geometric characteristics of the ellipsoid are used to search the path of obstacle avoidance, so as to realize the obstacle avoidance of UAV [14]. The obstacle avoidance beetle antenna search (OABAS) algorithm is a new path planning algorithm based on the biological heuristic algorithm, which is applied to the global path planning of UAV to achieve obstacle avoidance [15]. With the popularization of large-scale Internet of things (IOT) application, deep learning (DL) technology has become a promising method to improve the real-time obstacle detection and collision avoidance of highly autonomous UAV [16]. Iovino *et al.* [17] proposed a distributed flocking algorithm with obstacle avoidance capability for UAV swarming. It consists in an additional control added to solve both the limitation about the obstacles shape and the risk for the flock to come into the so called ''stuck situations''. The APF method is applied to the field of obstacle avoidance and collision avoidance of UAV, and satisfactory results are obtained in some researches. Pan *et al.* [18] combined the improved APF with PID algorithm, Wang *et al.* [19] combined the improved APF with collision prediction model, or realized the obstacle avoidance of UAV with bearings only measurement [20]. If the UAV companion is regarded as a dynamic obstacle [21], [22], or a dynamic APF [23] is established, the collision avoidance between UAVs can be solved in the improved APF [24]. To sum up, the APF method has good effect in route planning and obstacle avoidance, and is less used in cluster control. Moreover, few researchers have tried to overcome the local minimum problem of potential field caused by concave obstacles.

The cooperation between UAVs is an important factor to ensure the high quality of tasks. Zhang *et al.* [25], based on the consistency bundling algorithm, introduces the concept of asynchronous task allocation, and studies the task planning of UAV group in dynamic environment. The combination of virtual structure and path tracking method has a good performance in crowd collaborative control of mobile machines [26], [27]. The combination of virtual force method and rolling time domain method improves the efficiency of multi UAV cooperative search [28]. Shirani *et al.* [29], using Udwadia–kalaba method, proposed a distributed controller for collaborative task allocation of multiple UAVs. Andrade *et al.* Proposed a cooperative nonlinear model predictive control method for multiple UAVs using particle swarm optimization technology [30]. To solve the problem of UAV cooperative search task planning, Zhen *et al.* [31] and Huajun [32] proposed an ant colony algorithm based on APF using distributed architecture. Swarm intelligence algorithm is a good way to solve the optimization problem in a fixed environment [33], but the traditional swarm intelligence algorithm is difficult to track the changing optimal solution.

On the basis of the above research, in order to improve the success rate of multiple UAVs in mission execution, ensure good cluster control effect, and have flexible and changeable formation ability, this paper proposes a multi UAV cluster control method based on virtual core in improved APF, and realizes UAV cluster real-time path planning. The main contributions of this paper are as follows: 1) the concept of virtual core based on local potential field between UAVs is proposed. The location of virtual core is determined by k-means method, and the calculation of attractive field between UAVs is optimized. 2) a backtracking-filling method of APF is proposed, which solves the local minimum problem caused by compact concave obstacles in APF, and improves the APF method. 3) breaking through the fixed formation configuration, a UAV cluster formation control algorithm based on virtual core is proposed, which improves the cluster control effect and realizes the dynamic real-time flexible formation of multiple UAVs.

The structure of this paper is as follows: the second section introduces the problem description and APF method; the third section focuses on the multi UAV cluster control model and algorithm based on the improved APF method; the fourth section simulates and verifies the algorithm; the fifth part summarizes the work, points out the limitations of this paper and the future work.

II. PROBLEM DESCRIPTION AND APF PRINCIPLE

A. PROBLEM DESCRIPTION

On the basis of considering the maneuverability and threat avoidance requirements of UAV, this paper uses typical data elements such as obstacles and targets to establish the corresponding repulsion field and attraction field, and then analyzes the forces and motion of UAV group in the force field. Compared with the traditional method, the algorithm structure of APF method is clearer, the amount of intermediate data is relatively less, and the fault tolerance is higher. This method takes the track generated by global planning as the reference route, and quickly generates feasible route according to the dynamic change of flight environment, so as to ensure the safety of flight and the efficiency of mission execution.

This paper assumes that the UAV exists in the form of particles in the potential field. When there are many "particles" in a potential field, each particle can be regarded as a search individual in the three-dimensional search space and the current position of the particle is an input parameter of the track planning problem. The motion process of particles is the evolution process of the system. Particles have only two attributes: position and repulsion factor. Position is the relative position of particles in the potential field, and repulsion factor is the interaction factor of particles. Finally, the optimal

solution satisfying the termination condition is obtained by iterating and updating the position.

Aiming at the control mode of UAV cluster, this paper expects to achieve the following goals based on APF method: 1) the UAV can realize cluster flight by controllable formation. 2) the problem of local minimum of APF is overcome, especially for concave obstacles. 3) the UAV group successfully reaches the target point and completes the task. 4) fault tolerance or re import in the group can be realized.

Based on the analysis of the above cluster control objectives, a scheme of APF method for UAV cluster is proposed. The synthetic APF in space is the union of the repulsion field of obstacles, the attraction field of target points, the repulsion field between UAVs and the attraction field between UAVs. In the scheme, four kinds of APFs in space are classified first, then the force of UAV in each potential field is solved and superposed, finally the motion scheme of the UAV is calculated. Firstly, according to the action range of potential field internal force, the potential field in space is divided into two groups: inter-UAV potential field and global potential field. It is assumed that the attractive force and repulsion force generated by inter-UAV potential field are only valid within the range, and do not affect the global potential field. Because this grouping scheme is based on the action range of the force, from a global point of view, there is an intersection between the groups in the spatial position, which is not mutually exclusive. The force field satisfies the linear vector super-position mode, which can reduce the calculation load of the system. Secondly, the UAV is attracted or repulsed by the inter-UAV potential field, and is attracted by the target or repulsed by obstacles in the global potential field. The vector method is used to calculate the resultant force of the UAV at a certain point in space. In order to simplify the calculation of inter-UAV attraction field and improve the effect of cluster control, it is assumed that there is a virtual core of UAV cluster, and the position of the virtual core is calculated by k-means method to realize the formation flying around the core of multiple UAVs. Thirdly, the flight speed and direction of UAV are calculated by the mode value and phase angle of resultant force to realize the optimal path planning.

B. APF PRINCIPLE

Traditional simple APF is established by global calculation of obstacles in the system. With the known starting point, terminal point and obstacle location, an APF is constructed to imitate the existing potential energy mechanism in nature. The moving object in the environment is regarded as a particle in the APF, which moves in the APF established by the global calculation of obstacles. The virtual force field is obtained by negative gradient calculation. The virtual force field is composed of the attraction field towards the target point and the repulsion field far away from the obstacle.

The resultant potential field is calculated according to the following equations:

$$U(q) = U_{att}(q) + U_{rep}(q) \tag{1}$$

$$F(q) = -\nabla U(q) \tag{2}$$

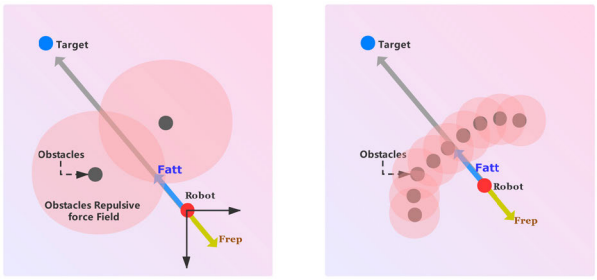

FIGURE 1. Local minimum in APF: (a) Sparse obstacles; (b) Dense concave obstacles.

The position of particle in space is $q(x, y, z)$, and the classical attraction potential function is:

$$U_{att}(Q) = \frac{1}{2}\xi\rho^2\left(q, q_{goal}\right) \tag{3}$$

where ξ is the scale factor of attraction, $\rho\left(q, q_{goal}\right)$ is the relative distance between the particle and the target q_{goal}. The corresponding attraction $\boldsymbol{F}_{att}(q)$ is the negative gradient of the potential field function of the target, and the direction points to the point of the target. In the process of the UAV flying to the target point, the attraction converges to zero linearly.

$$\boldsymbol{F}_{att}(q) = -grad\left[U_{att}(q)\right] \tag{4}$$

The classical obstacle repulsion potential function is:

$$U_{rep}(Q) = \begin{cases} \frac{1}{2}\eta\left[\frac{1}{\rho(q, q_{obs})} - \frac{1}{\rho_0}\right]^2 & \rho \le \rho_0 \\ 0 & \rho > \rho_0 \end{cases} \tag{5}$$

where η is the scale factor of attraction, $\rho(q, q_{obs})$ is the relative distance between the particle and the obstacle q_{obs}, and ρ_0 is the radius of influence of the repulsive force of the obstacle. The corresponding repulsive force $\boldsymbol{F}_{rep}(q)$ is the negative gradient of the target potential field function.

$$\boldsymbol{F}_{rep}(q) = -grad\left[U_{rep}(q)\right] \tag{6}$$

C. THE LOCAL MININUM PROBLEM OF APF METHOD AND ITS IMPROVEMENT ANALYSIS

The traditional APF method has the problem of local minimum. On the premise that the potential energy of the target point is not the global minimum or there is a local minimum in the global potential field, when the UAV reaches the local minimum position with the guidance of the potential field, it probably cannot escape from the area, which leads to the failure of route planning. The local minimum in the APF can be divided into two cases, as shown in Figure 1.

In Figure 1a, at the intersection of the repulsive field boundaries of two obstacles, if the resultant force on the UAV is exactly zero, the UAV will fall into the local minimum of the APF. In order to avoid this local minimum phenomenon,

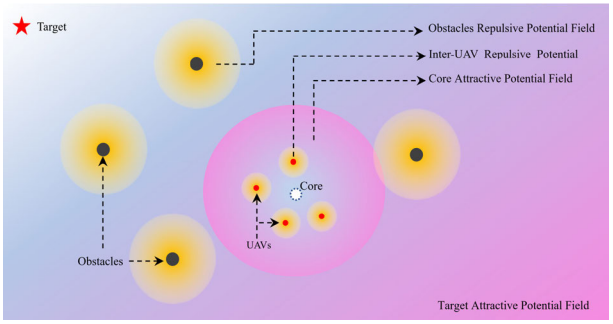

FIGURE 2. Schematic diagram of APF.

a disturbance component is introduced into the attraction field of the target point, which directly affects the attraction generated by the target point. When the UAV falls into the local minimum point, the speed of the UAV will be reduced to a relatively small range. When this low speed state is maintained for a certain period of time, the disturbance component will start to affect the attraction. The increase of attraction will readjust the local minimum value of APF, so that the UAV can escape from the original local minimum value point.

In the process of UAV running from the starting point to the terminal point, when encountering the compact concave obstacles as shown in Figure 1b, the above method to solve the local minimum value will be invalid. Because with the increase of disturbance component, UAV is getting closer to the obstacle, but it can't pass through the dense obstacle, so the UAV can't escape from the local minimum. In order to solve this local minimum problem, we propose a backtracking-filling algorithm. The main idea of this method is as follows: after the UAV falls into the local minimum value, it will return to a certain point in the previous path, and then fill the local minimum point with virtual obstacles to update the original obstacle potential field, so that the UAV will not fall into the local minimum again.

III. MATHEMATICAL MODEL

The map of the single potential field (global and UAV related) and their union is shown in Figure 2. The attraction field of the target point is a global potential field. The farther away from the target point, the stronger the attraction field intensity is. The attraction field of the virtual core is a local potential field, and its intensity increases with the increase of the distance from the core. The repulsive field of the obstacle or the inter-UAV is a smaller local potential field. The potential field strength of repulsion field decreases gradually from the center to the outside. In Figure 2, the darker the color is, the stronger the potential field intensity is.

Set the number of UAVs to be dispatched as N, divide the UAVs into k different groups according to the task requirements, and record the u-th group as G_u,where $u = 1, 2, 3, \ldots, k$, and the number of drones in u-th group is N_u. The movement of the UAV in the potential field when the number of groups is 1 is analyzed, and the state of the UAV at this time is described as a single group model. According to the movement of the UAV in potential field when the number of teams is more than 1, the state of the UAV at this time is described as a multi group model.

The forces on the UAV in the group G_u are defined as follows:

$\boldsymbol{F}_{G-rep}$: The inter-UAV repulsion force drives UAVs in the same group to separate from each other to avoid collision between them. $\boldsymbol{F}_{G-rep}$ has a range of action ρ_0, when $\rho > \rho_0$,$\boldsymbol{F}_{G-rep} = 0$.

$\boldsymbol{F}_{GC-att}$: The UAVs in the group G_u are attracted by the virtual core of the group to ensure that they can maintain the trend of convergence.

$\boldsymbol{F}_{new-att}$: The attraction of the target point on the UAV is calculated by the improved APF method to ensure that each UAV can move towards the target.

$\boldsymbol{F}_{rep}$: The combined repulsion force generated by all obstacles in the APF drives the UAV to avoid obstacles.

$\boldsymbol{F}_{Ov-rep}$: The repulsion force between the current UAV and the v-th obstacle, with the action range ρ_1. When $\rho > \rho_1$, $\boldsymbol{F}_{Ov-rep} = 0$.

A. ATTRACTIVE FORCE CALCULATION AND SIMPLIFICATION BETWEEN UAVS

Any two UAVs in the same group G_u have mutual attraction, and the attractive force ensures that the two UAVs cannot be separated from the team. Let $q\,(x, y, z)$ be the position of a UAV in space Q in the group G_u, where $q_1 q_2 \ldots q_n \in G_u$, n is the number of UAVs in the u-th group G_u, then the directional distance between the i-th UAV and the j-th UAV is represented by $\boldsymbol{\rho}_{ij} = \rho\left(q_i, q_j\right)$. $\boldsymbol{\rho}_{ij}$ satisfies the following equation:

$$\left|\boldsymbol{\rho}_{ij}\right| = \sqrt{(x_i - x_j)^2 + (y_i - y_j)^2 + (z_i - z_j)^2} \tag{7}$$

Then the attractive potential field function of the i-th UAV generated by the j-th UAV at the point q_i is as follows:

$$U_j^{att}(i) = \frac{1}{2}\xi \cdot \boldsymbol{\rho}_{ij}^2 \tag{8}$$

where ξ is the proportion factor of the inter-UAV attraction. The attractive force of the i-th UAV generated by the j-th UAV at point q_i is as follows:

$$\boldsymbol{F}_j^{\text{att}}(i) = -\nabla U_j^{att}(i) = \xi \cdot \boldsymbol{\rho}_{ij} \tag{9}$$

Therefore, the attractive forces between a group of UAVs at the same time can be expressed as:

$$\boldsymbol{F}_{ij} = \begin{vmatrix} 0 & \boldsymbol{F}_{12} & \boldsymbol{F}_{13} & \ldots & \boldsymbol{F}_{1n} \\ \boldsymbol{F}_{21} & 0 & & & \ldots \\ \boldsymbol{F}_{23} & \ldots & 0 & & \ldots \\ \ldots & & & \ldots & \ldots \\ \boldsymbol{F}_{2n} & \ldots & \ldots & \boldsymbol{F}_{(n-1,n-1)} & 0 \end{vmatrix} \tag{10}$$

where $\boldsymbol{F}_{ij} = \boldsymbol{F}_j^{\text{att}}(i)$. So, the combined attractive force of the i-th UAV at point q_i by other UAVs in group G_u is:

$$\boldsymbol{F}_{att}(i) = \sum_{j=1}^{n} \boldsymbol{F}_j^{att}(i) \tag{11}$$

When calculating the attractive force between UAVs, a UAV needs to obtain the location information of all UAVs in its

group at the same time. The complexity of data exchange in each control cycle is $O(N^2)$, which has higher requirements for data exchange and is not convenient for distributed management. At the same time, in view of the single UAV failure, the traditional data transmission mode cannot timely feedback and update the UAV failure status, which may cause the global calculation abnormal. We ropose the concept of virtual core to simplify the traditional attractive field between UAVs.

If the virtual core position is set as $q_{\text{core}}(x_0, y_0, z_0)$, then the attractive potential field function generated by the virtual core at the point of q_i is as follows:

$$U_{core}^{att}(i) = \frac{1}{2}\xi \cdot \boldsymbol{\rho}^2(i, core) \tag{12}$$

The attractive force is:

$$\boldsymbol{F}_{core}^{att}(i) = \xi_0 \cdot \boldsymbol{\rho}|_{\boldsymbol{\rho}=\rho_{(i,core)}} \tag{13}$$

Order $\boldsymbol{F}_{core}^{att}(i) = \boldsymbol{F}_{att}(i)$,to exit (x_0, y_0, z_0) and ξ_0.

In the group G_u, there must be a point $q_{\text{core}}(x_0, y_0, z_0)$ that holds the equation $\forall \boldsymbol{F}_{core}^{att}(i) = \boldsymbol{F}_{att}(i)$ forever. Then set point q_{core} is the virtual center of the group G_u. Therefore, the $\boldsymbol{F}_{att}(i)$ of the i-th UAV calculated in the force field can be reduced to $\boldsymbol{F}_{core}^{att}(i)$. Where $\boldsymbol{F}_{core}^{att}(i)$ is the attraction value of the i-th UAV calculated from the attraction field generated by the geometric center $q_{\text{core}}(x_0, y_0, z_0)$ of the group G_u.

In order to determine the virtual core of regional potential field more conveniently, we use the k-means method to calculate the center position and range. This is a classical algorithm to solve the clustering problem. In this method, N objects are divided into K clusters, and the center of each cluster is represented by the mean value of the objects in the cluster, which is iterated many times until the objects in each cluster no longer change. At this time, the square error criterion function is optimal, that is, the similarity of objects in the cluster is high, and the similarity between clusters is low. With this method, N UAVs in space can be divided into K groups quickly, and the virtual core of each cluster can be calculated.

The process of the UAV clustering and virtual core of each cluster iterative calculation is described as follows:

1) Among the N objects, K objects are randomly selected to represent the initial position mean or geometric center of K clusters.
2) Calculate the Euclidean distance between the rest of the objects and the centers of the above clusters. According to the principle of closest distance center, the rest of the objects are automatically added to the cluster with the shortest distance. Update the composition of each cluster last time, and iterate out new K clusters.
3) The average position of all objects in each cluster is calculated as the center of each cluster after iteration. This center is the virtual core of the current cluster.
4) Repeat step 2) 3) until the center of each cluster converges to its fixed position, and the clustering ends. At the same time, the virtual core of each group is determined.

According to the principle of nearest distance center, the distance measurement equation is as follows:

$$d(x_1, x_2) = \sqrt{\sum_{i=1}^{n}(x_{1i} - x_{2i})^2} \tag{14}$$

where x_1, x_2 represents two n-dimensional data objects, and $d(x_1, x_2)$ represents the distance between x_1 and x_2. According to Euclidean distance, the distance between each data object and each cluster center is calculated. The k-means algorithm uses the square error criterion function to evaluate the clustering performance, that is to say, after clustering, all clusters are evaluated by the equation. The selection equation of criterion function is as follows:

$$E = \sum_{i=1}^{k}\sum_{p\subset G_u}|p - C_u|^2 \tag{15}$$

where E is the sum of the square errors of all the objects in the database, p is the given data object, and C_u is the mean value of cluster G_u.

The mean value of all objects in each cluster is used as the cluster center, and the calculation equation of the cluster center is as follows:

$$C_u = \frac{1}{n}\sum_{p\subset G_u} p \quad u = 1, 2, 3 \ldots k \tag{16}$$

Inspired by the clustering problem, k-means algorithm is used to find the virtual core of a group of UAVs, simplify the inter-UAV machine attractive force in APF, and reduce the complexity of data exchange in each control cycle. The UAV is constrained by virtual core attractive force, and realizes cluster flight in APF. In addition, this method can flexibly provide cluster grouping, task allocation, track planning and other schemes by adjusting the calculation logic and parameters of k-means algorithm for hundreds of UAV groups. It has good performance in the intelligent, adaptive and redundancy reduction of the system.

B. REPULSION BETWEEN UAVS

Any two UAVs in the same group G_u have mutual repulsion. The repulsion force between UAVs ensures a certain distance between UAVs and avoids the collision between UAVs. The directional distance between the two UAVs is represented by $\boldsymbol{\rho} = \rho(q_1, q_2)$.

$$U_{rep}(q) = \begin{cases} \frac{1}{2}\cdot\eta\cdot\left[\frac{1}{|\boldsymbol{\rho}|} - \frac{1}{\rho_0}\right]^2 & \rho \le \rho_0 \\ 0 & \rho > \rho_0 \end{cases} \tag{17}$$

where η is the gain coefficient of repulsion, ρ_0 is a constant representing the influence distance of repulsion force. The repulsion force is the negative gradient of the repulsion field, and the direction is far away from the UAV as a dynamic obstacle. The position of the current i-th UAV is set as q_i, and the position of the j-th UAV as a dynamic obstacle is set as q_j.

Then, when $q \neq q_{\text{goal}}$, the repulsion force $F_i^{rep}(q_j)$ of the i-th UAV caused by the j-th UAV can be written as follows:

$$\boldsymbol{F}_i^{rep}(q_j) = -grad\left[U_{rep}^j(q_i)\right] = \begin{cases} \boldsymbol{F}_{reij} & \rho \le \rho_0 \\ 0 & \rho > \rho_0 \end{cases} \quad (18)$$

$$F_{reij} = \eta \cdot \left[\frac{1}{|\boldsymbol{\rho_{ij}}|} - \frac{1}{\rho_0}\right] \cdot \frac{1}{|\boldsymbol{\rho_{ij}}|^2} \quad (19)$$

where $U_{rep}^j(q_j)$ is the repulsion field function generated by the j-th UAV, and the vector $\boldsymbol{F}_{reij}$ is from the j-th UAV to the i-th UAV.

At the same time, the repulsion force of the i-th UAV caused by the repulsion field of other UAVs is:

$$\boldsymbol{F}_{G-rep}(i) = \sum_{j=1}^{n} F_{repj}(i) = \sum_{j=1}^{n} F_{reij} \quad (20)$$

C. ATTRACTION OF TARGET POINT TO UAV

The UAV is attracted by the target point in the potential field, which enables the UAV to shuttle between the peaks and troughs formed by obstacles and advance towards the target point. The directed distance between the UAV and the target point $q_{goal}(x_0, y_0, z_0)$ is expressed by $\boldsymbol{\rho}_{goal}(i) = \rho\left(q_i, q_{goal}\right)$, then the attractive potential field function generated by the target point q_{goal} at q_i is as follows:

$$U_{att}(i) = \frac{1}{2}\xi \cdot \boldsymbol{\rho}_{goal}^2(i) \quad (21)$$

where ξ is the attractive scale factor. The attractive force produced by the target point q_{goal} at point q_i is as follows:

$$\boldsymbol{F}_{att}(i) = -grad\left[U_{att}(i)\right] = \xi \cdot \rho|_{\boldsymbol{\rho}=\boldsymbol{\rho}_{goal}(i)} \quad (22)$$

D. REPULSION BETWEEN UAV AND OBSTACLE

It is assumed that the directional distance between the i-th UAV and obstacle O is represented by $\boldsymbol{\rho_{iO}} = \rho(q_i, O)$. Then, the repulsion field intensity generated by obstacle O at point q_i of the i-th UAV is as follows:

$$U_{rep}(q) = \begin{cases} \frac{1}{2} \cdot \eta \cdot \left[\frac{1}{|\boldsymbol{\rho}|} - \frac{1}{\rho_0}\right]^2 \cdot \rho^{\sigma}(q, q_{goal}) & \rho \le \rho_0 \\ 0 & \rho > \rho_0 \end{cases} \quad (23)$$

where η is the repulsion gain coefficient and ρ_0 is a constant representing the influence distance of obstacles. σ is an arbitrary constant greater than zero, which is used to introduce the relative distance between the UAV and the target point, so as to ensure the global minimum of the whole potential field only at the target point q_{goal}. The repulsion force is the negative gradient of the repulsion field, and the direction is away from the obstacles. Relative to the i-th UAV, Set the v-th obstacle as O_v, where $v = 1, 2, 3 \ldots, V$. When $q \neq q_{\text{goal}}$, the repulsive force $F_i^{rep}(O_v)$ of the i-th UAV caused by obstacle O_v can be written as follows:

$$\boldsymbol{F}_i^{rep}(O_v) = -grad\left[U_{rep}(O_v)\right] = \begin{cases} \boldsymbol{F}_{reiov} & \rho \le \rho_0 \\ 0 & \rho > \rho_0 \end{cases} \quad (24)$$

$$F_{reiov} = \eta \cdot \left[\frac{1}{|\boldsymbol{\rho_{io}}|} - \frac{1}{\rho_0}\right] \cdot \frac{1}{|\boldsymbol{\rho_{io}}|^2} \cdot \rho^{\sigma}(q, q_{goal}) \quad (25)$$

where $U_{rep}(O_v)$ is the repulsion field function generated by obstacle O_v, and the vector $\boldsymbol{F}_{reiov}$ points from obstacle O_v to the i-th UAV.

At the same time, the resultant force of repulsion force on the i-th UAV generated by repulsion field of V obstacles is:

$$\boldsymbol{F}_{O-rep}(i) = \sum_{Ov=1}^{V} \boldsymbol{F}_i^{rep}(O_v) = \sum_{Ov=1}^{V} F_{reiov} \quad (26)$$

The state of APF is updated by combining the original APF with distributed information. The obstacle information and position information fed back by all UAVs in the whole system are collected in real time through the central control system. The UAV obtains the relative position of the obstacle target through the visual image data, and then converts it into geographic coordinates. The central operating system obtains the obstacle coordinates, and updates the potential field status.

The specific coordinate updating method is as follows:

UAV calculates the length, width and height information of obstacles through current position information and visual depth sensor. The obstacle information is the cross-section information of UAV's direction. Through the current depth data, the UAV rotates the obstacle information into the end-point information in the UAV coordinate system and uploads it to the cloud server. According to the coordinates of end-point location information and the UAV location information, the cloud server service program constructs cuboid obstacles. The obstacle section is L in length, W in width and H in height. According to the obstacle information, the cloud service program divides the cuboid into small cuboids. The length, width and height of the small cuboid are l, w, h. The obstacles are divided into basic units. The cloud service program takes a, b, c obstacle points on the length, width and height of the obstacles respectively. Taking the length direction as an example, the number of obstacle points is calculated by the following equation. Then the global potential field is updated according to the obstacle points.

$$a = \left[\frac{L}{l}\right] \quad (27)$$

E. THE METHOD TO OVERCOME LOCAL MINIMUM

In this paper, we consider that there are two kinds of local minimum problems in the traditional APF method, which are caused by sparse obstacles and dense concave obstacles. In the flight process of UAV, the reason of local minimum value is judged by searching the number of obstacles around, and then different methods are used to make the UAV escape from the local minimum value.

In order to solve the local minimum problem caused by sparse obstacles in APF, the disturbance component is introduced into the attraction field of target point, and the following improved design is carried out:

$$\boldsymbol{F}_{new-att}(q) = \left(\mu_p + \mu_t\right) \cdot \boldsymbol{F}_{att}(q) \quad (28)$$

where μ_p is the positive weight factor, which means that the attraction of the current target increases with the increase of the target distance, so as to ensure that the UAV can fly along the reference route in the case of no new threat. μ_t is the time disturbance component weight factor of the target attractive force. When the speed of UAV is in the normal range, the value of μ_t is zero. When the speed of UAV is reduced to a certain range and the state is maintained for a certain time, the value of μ_t increases with time. The disturbance component μ_t is defined as follows:

$$\mu_t = \begin{cases} \int_{t_0}^{t} \varepsilon d\,(t)\,\{t > t_0, d\rho/dt < v_0\} \\ 0 \end{cases} \tag{29}$$

In order to solve the local minimum problem caused by dense concave obstacles in APF, a backtracking-filling method is proposed. The implementation steps of this method are as follows:

1) Judge and determine the local minimum value of UAV falling into dense obstacle.
2) Determine the location of the obstacle with the minimum distance to the UAV.
3) Taking the obstacle point as the center, a virtual obstacle with radius of R1 is placed, and then the APF is updated.
4) UAV group location backtracking. Each UAV in the group will return to the position on its own path where the distance from any obstacle in the potential field is greater than R2.
5) Continue the APF method.

Among them, step 1) can be evaluated by the number of obstacles in a certain range around the UAV by searching. Step 4) ensure that each UAV can avoid the new virtual obstacles. R1 is the radius of virtual obstacle, which is determined by UAV detection radius, obstacle repulsion radius and repulsion coefficient. R2 is the backtracking coefficient, which is determined by R1, the repulsion radius of the obstacle and the repulsion coefficient.

Using the APF method based on virtual core, the UAVs in the group can fill virtual obstacles at the local minimum value of the original potential field respectively when the UAV cluster performs tasks, which improves the efficiency of path planning in the updated APF.

F. THE RESULTANT FORCE OF UAV AND PARAMETRIC CONSTRAINT EQUATIONS

In order to ensure the moving object moving towards the target point, the component of repulsion force in the direction of attractive force is required to be smaller than that of attractive force, and the next track point is closer to the target point than the previous one. From these two conditions, the constraint equation of the two-dimensional space track planning parameters can be deduced.

Let the $\boldsymbol{F}_{att}$ be the attractive force, the $\boldsymbol{F}_{rep}$ be the repulsive force, δ be the step length, and θ be the angle between the attractive force and the repulsive force. The component of vector $\boldsymbol{F}_{rep}$ in the direction of $\boldsymbol{F}_{att}$ is $\boldsymbol{F}_{rep} \cdot \cos\theta$. In order to ensure that the aircraft flies towards the target point, when $\theta \leq \pi/2$, the UAV can fly towards the target point; when $\theta > \pi/2$ it must meet the following requirements:

$$F_{rep} \cdot cos\theta < F_{att} \tag{30}$$

Let the distance between the current position (x, y) of the UAV and the target point (x_{goal}, y_{goal}) be ρ. In order to ensure that every step of the UAV is closer to the target point, that is, $\rho_{new} < \rho$.

In order to ensure that the UAV flies to the target point, the range of the attractive coefficient k_{att} can be obtained by using the attraction equation as follows:

$$k_{att} > F_{rep} \cdot \frac{\cos\theta}{\rho\,(x, x_{goal})} \tag{31}$$

All the attractive forces and repulsive forces on the UAV are decomposed to x and y axes respectively to obtain $F_{ax}, F_{ay}, F_{rx}, F_{ry}$. The resultant force of the UAV is:

$$F = (F_{ax} + F_{rx})^2 + (F_{ay} + F_{ry})^2 \tag{32}$$

Then the increment of UAV in x and y directions are as follows:

$$x_{new} = x + \delta \cdot \frac{F_{ax} + F_{rx}}{F}, \quad y_{new} = y + \delta \cdot \frac{F_{ay} + F_{ry}}{F} \tag{33}$$

By substituting the inequality $\rho_{new} < \rho$, we get:

$$\delta < 2(1 + k)\frac{Fa}{F}\rho\,(x, x_{goal}) \tag{34}$$

where $k_{att} = \min(k_x, k_y)$, k_x, k_y are the scale factors:

$$F_{rx} = k_x F_{ax}, F_{ry} = k_y F_{ay} \tag{35}$$

In order to ensure that every step of UAV planning is closer to the target point, the component of repulsion force in x and y direction is required to be smaller than the attractive force component. Route planning parameters shall meet the following constraints:

$$\begin{cases} \delta < 2(1 + k_{att})\dfrac{F_{att}}{F}\rho\,(x, x_{goal}) \\ k_{att} > F_{rep} \cdot \dfrac{cos\theta}{\rho\,(x, x_{goal})} \end{cases} \quad \theta > \pi/2 \tag{36}$$

IV. SIMULATION AND ANALYSIS

In order to verify the effectiveness of the improved APF method based on virtual core in the control of multiple UAVs, we design a simulation experiment based on the physical model of quad-rotor UAV. Compared with fixed wing UAV, smart car and other agents, quad-rotor UAV has faster response speed, especially in lateral movement. In the following, UAV refers to quad-rotor UAV. In the simulation, we use the mass free and volume free protons to simulate the UAV. Considering the actual volume of UAV, the minimum safety interval is set in the algorithm. The simulation experiment uses MATLAB platform, the computer processor is Intel Xeon e3-1230 v5 @ 3.4GHz, the memory is 16GB, and the system is windows 10 professional.

TABLE 1. Parameter values and definitions of the APF.

Parameter	Value	Definition
K_{goal_att}	0.5	Target attractive gain coefficient
K_{core_att}	4	Core attractive gain coefficient
$Mobs$	2.6	Obstacle repulsive gain coefficient
$Dobs$	4	Repulsive radius
$Muav$	2.2	Inter-UAV repulsive gain coefficient
$Duav$	2.5	Inter-UAV repulsive radius
L	0.05	UAV operation step length

The attraction gain coefficient of target point determines UAV's tendency UAV to the target point. If the figure is too small, the UAV will not be able to reach the target point. The core attraction gain coefficient determines the tendency of multiple UAVs aggregation. If the figure is too small will lead to poor UAV cluster effect. The gain coefficient and action radius of the repulsion force of obstacles determine the safe distance between the UAV and the obstacle. If the figure is too small, the UAV will collide with the obstacle. The gain coefficient and action radius of repulsion force between UAVs determine the repulsion force, safety distance and group uniformity between UAVs. If the figure is too small repulsion force will lead to collision between UAVs. The moving step length of the UAV refers to the maximum running distance of UAV in each iteration, which determines the running speed and obstacle avoidance accuracy of the UAV. The setting of motion step size is limited by the computing speed of the computer. If the movement step size is too large, the cluster control and path planning cannot be carried out effectively.

The simulation performance of the algorithm is described in two simulation scenarios: self-built APF and real scene conversion APF. The simulation results include: 1) the basic performance of the model. The force data of UAV are analyzed. The simulation results show that three UAVs have successfully completed the mission by controlling the flight in clusters. 2) performance of the virtual core. The distance between UAV and virtual core is analyzed. By changing the four factors of inter-UAV attraction, repulsion, starting point position of and target point position, the performance of virtual core algorithm in multi UAV cluster control is demonstrated by using the method of limited variable simulation. 3) cluster reconfiguration performance. The simulation results show the flight effect of cluster reconfiguration when a UAV fails or a new UAV joins in the flight process. 4) simulation analysis of backtracking-filling method. The simulation results of UAV escaping from the local minimum point in the APF with dense concave obstacles are given. 5) simulation results of real scene. This paper presents the effect of cluster flight and mission execution in the APF simulation scene of the National Olympic Village in Beijing.

A. MODEL FOUNDATION PERFORMANCE ANALYSIS

1) SIMULATION SCENE

In this paper, the APF is established in the area of 100m times 100m. In this area, 1000 times 1000 grids are defined in steps of 0.1m. Three groups of randomly distributed irregular obstacles are set in the potential field, and multiple evenly distributed sampling points are set on each obstacle. On each grid, the repulsion force generated by all sampling points of an obstacle is calculated and superposed, and the combined repulsion force of the obstacle at this grid is obtained. Then the repulsion field of the whole area can be approximately expressed as a two-dimensional matrix of the repulsion modulus of all the obstacles on all the grids, and then the APF model of irregular obstacles is established.

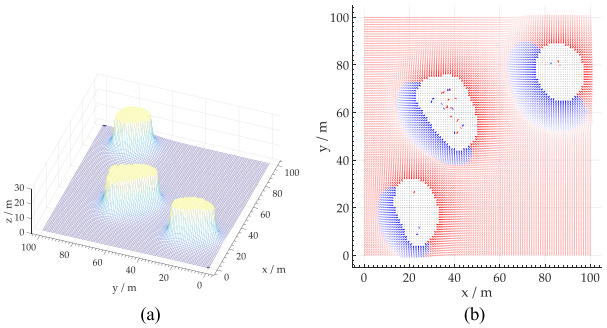

FIGURE 3. APF of irregular obstacles: (a) 3D visualization model;(b) Direction of resultant force in cross section of APF.

Firstly, the direction of the resultant force applied on the UAV is analyzed to guide the UAV path planning. Secondly, when two UAVs are performing tasks, the distance between them and the force data of each UAV are obtained by simulation. Finally, when three UAVs are performing tasks, the cluster effect and the results of target tasks are obtained by simulation.

2) SIMULATION RESULTS

Figure 3 shows the APF of irregular obstacles. In Figure 3a, the height of the protuberance in the potential field represents the size of the repulsion field. The color changes from dark to light, which means the repulsion field changes from weak to strong. In the potential field, the x-axis direction and y-axis direction are 100m respectively, and the minimum potential grid is 1m times 1m.

In a cross section of the potential field, with (0,0) as the starting point and (95,97) as the target point of the UAV's mission, through the comprehensive analysis of the repulsion force of the obstacles in the potential field to the UAV and the attraction of the target point to the UAV, the resultant force direction diagram of the UAV is obtained, as shown in Figure 3b. In Figure 3b, the red area represents the resultant force of the trend target point, the blue area represents the resultant force of the departure obstacle, and the depth of color represents the magnitude of the resultant force. After the UAV takes off from the starting point, it mainly moves in the direction guided by the resultant force of the red area. When approaching the obstacle, the UAV will fly along the canyon at the junction of red and blue areas. Under the action of the resultant force, the UAV track planning is realized and reaches the target task point.

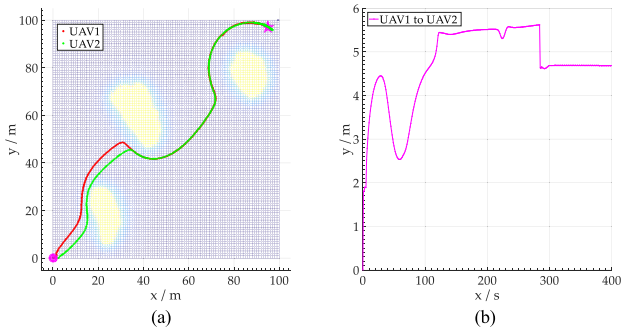

FIGURE 4. Cooperative flight of two UAVs: (a) 2D track visualization; (b) Distance between two UAVs.

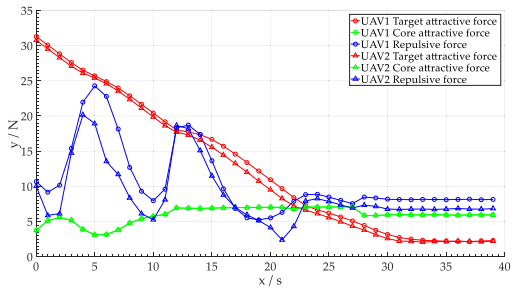

FIGURE 5. Forces on UAVs.

Taking two UAVs as an example, the force of UAV during flight is analyzed. Two UAVs start from (0,0) and fly to (95,97) target point. It can be seen from Figure 4a that the two UAVs reach the target point in the form of maneuvering formation. Figure 4b shows the change curve of the distance between two UAVs with the flight time. The distance between the two UAVs is stable at about 5m, which reflects the control effect of mobile formation based on virtual core.

Figure 5 shows the force situation of two UAVs in the potential field during the mission execution. Among them, the red line indicates the attractive force by the target point to the UAV, the green line indicates the attractive force by the virtual core to the UAV, the blue line indicates the combined repulsion force by all other objects to the UAV. In the process of mission flight, the forces of two UAVs are basically the same, which can be extended to the mutual forces of multiple UAVs, thus reflecting the effectiveness of cluster control method based on virtual core.

Three UAVs take off from (0,0), fly around the irregular obstacles, and go to the target point (95,97) to perform the task. The navigation trace and task execution effect are shown in Figure 6. According to the 3D simulation results, the three UAVs not only keep the formation around the virtual core, but also have high maneuverability in the formation, which shows excellent cluster control effect.

B. VIRTUAL CORE PERFORMANCE ANALYSIS

1) SIMULATION SCENE

In the scene of irregular obstacle potential field in Figure 3, control variable method is used to carry out multiple

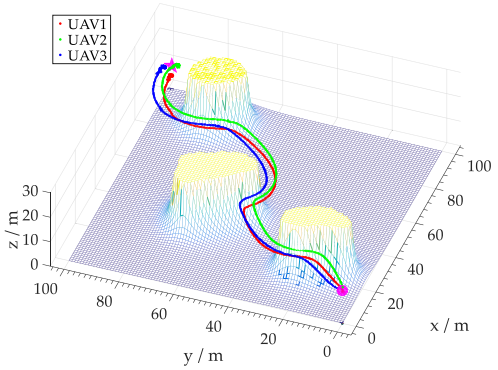

FIGURE 6. 3D simulation of three UAVs performing tasks.

comparative simulation experiments to verify the performance of virtual core. Variable factors include: inter-UAV repulsion force, virtual core attraction, starting position of each UAV.

Firstly, for three UAVs taking off from the same starting point to perform tasks, the following four aspects are compared and simulated: whether there is rejection between UAVs, whether virtual core is attractive to the UAV. Secondly, for three UAVs taking off from different starting points to carry out tasks, the following four aspects are compared and simulated: whether there is rejection between UAVs, whether virtual core is attractive to the UAV. The function of virtual core is analyzed by the task completion and the data of distance between UAVs. Finally, by analyzing the distance from each UAV to the virtual core, the cluster formation effect and maneuverability of the control algorithm are verified.

2) SIMULATION RESULTS

When three UAVs take off from the same starting point under different forces conditions, Figure 7 shows the 2D visual task execution process, Figure 8 shows the variation curve of the distance between UAVs.

The comparative analysis is as follows: 1) when there is no repulsion force between UAVs, Figure 7a and Figure 7c show that the flight path of UAVs basically coincides shortly after takeoff. Figure 8a and Figure 8c show that the minimum distance between aircrafts is 0.3m or 0m, which is far less than the minimum safety distance. After taking off, UAVs collided with each other, and the mission could not be completed. 2) when there is repulsion between UAVs, but there is no attraction of virtual core to UAVs, Figure 7b shows that although some UAVs have the possibility of completing tasks, the formation flying is disordered. Figure 8b shows that the distance between drones fluctuates in a large range from 10m to 45m, without cluster effect. 3) when the UAV has both repulsion and core attraction, Figure 7d shows that the UAV can complete the task, and Figure 8d shows that the distance between UAVs is about 6m, which fluctuates in a small range compared with figure 8b, with obvious clustering effect and mobile formation characteristics. When multiple UAVs take off from the same starting point to perform tasks,

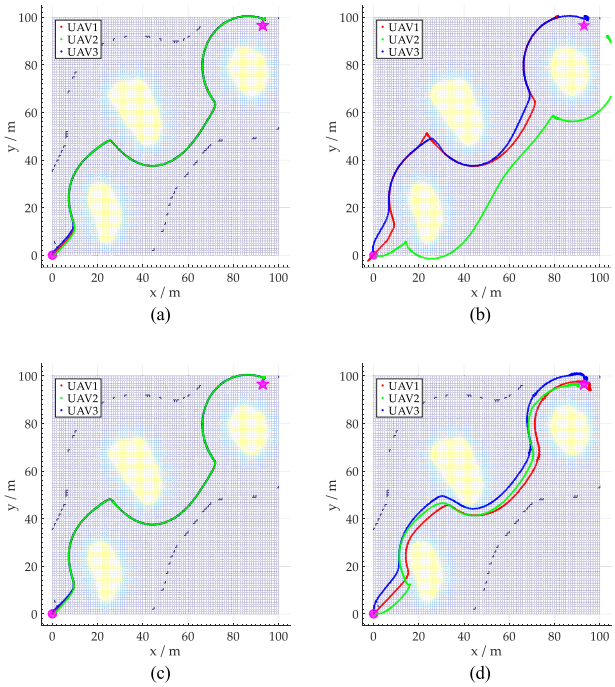

FIGURE 7. 2D visualization of task execution process with different forces at the same starting point: (a) No repulsion and no core attract-tion; (b) Repulsion but no core attraction; (c) No repulsion but core attraction; (d) Repulsion and core attraction.

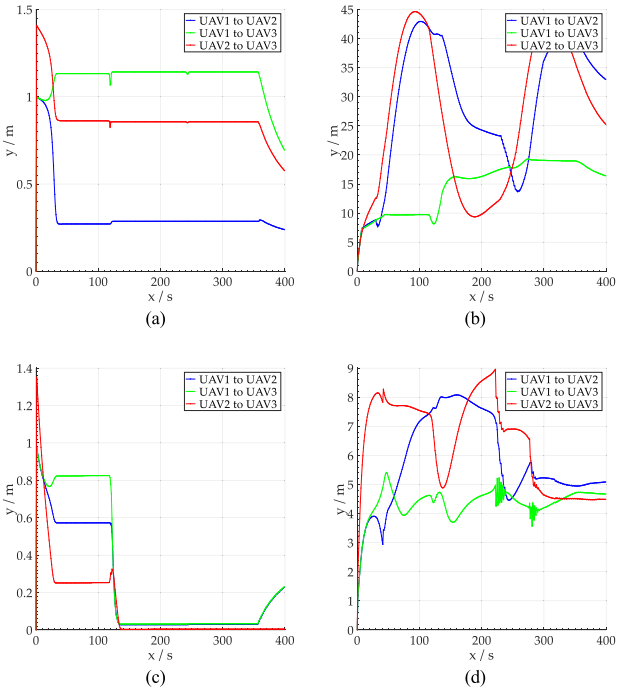

FIGURE 8. UAV spacing during different force tasks from the same starting point: (a) No repulsion and no core attraction; (b) Repulsion but no core attraction; (c) No repulsion but core attraction; (d) Repulsion and core attraction.

the core attraction ensures the cluster control effect, improves the success rate of task execution, and improves the cluster maneuver performance.

When three UAVs take off from the different starting points under different forces conditions, Figure 9 shows the 2D

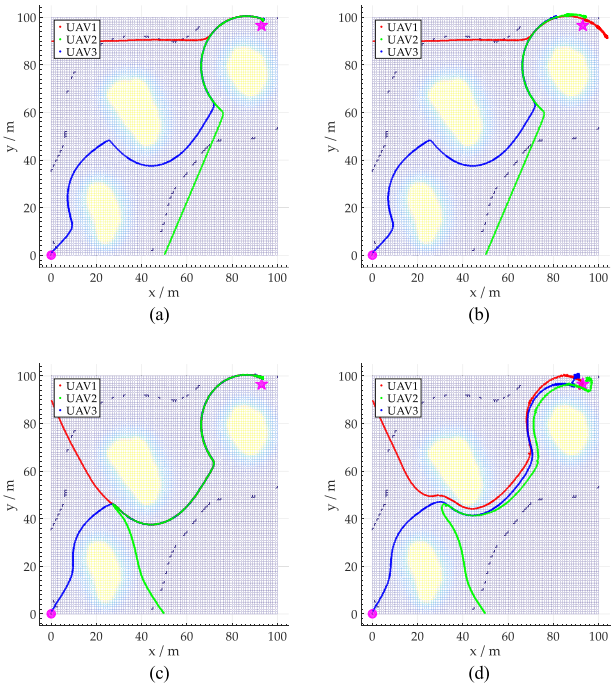

FIGURE 9. 2D visualization of task execution process with different starting points and different forces: (a) No repulsion and no core attract-tion; (b) Repulsion but no core attraction; (c) No repulsion but core attraction; (d) Repulsion and core attraction.

visual task execution process, Figure 10 shows the variation curve of the distance between UAVs.

The comparative analysis is as follows: 1) when there is no repulsion force between UAVs, Figure 9a and Figure 9c show that after the UAV group takes off, whether there is core attraction or not, the flight path will coincide before reaching the target point. Figure 10a and Figure 10c show that the distance between aircrafts after the flight path is overlapped is close to or equal to 0 m, far less than the minimum safe distance. The mission could not be completed due to the collision of UAVs. 2) when there is repulsion but no core attraction between UAVs, Figure 9b shows that UAVs finally reach the target point. However, the three UAVs fly independently, and the termination point is a certain distance from the target point, so there is a greater risk of mission failure. Figure 10b shows that the distance between UAVs decreases gradually in the course of flying towards the target point, and finally fluctuates in a wide range of 20-30 m without cluster effect. 3) when the UAV has both repulsion and core attraction, Figure 9d shows that the UAV can complete the task. Figure 10d shows that the distance between UAVs is basically stable at about 6m, which proves the effectiveness of the algorithm in terms of cluster effect and formation mobility.

After taking off from (0,0), the three UAVs fly around the irregular obstacles and go to the target points (95,97) to perform tasks. Figure 11 shows the flight path, UAV cluster flight effect and mission completion. In Figure 11, the black line represents the trajectory of the virtual core during flight. In the whole process of mission execution, three UAVs have

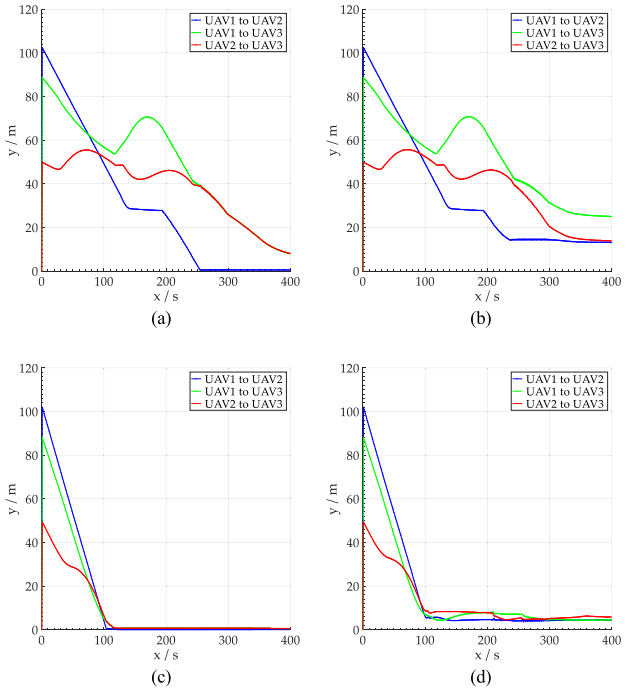

FIGURE 10. UAV spacing during task execution with different starting points and different forces: (a) No repulsion and no core attraction; (b) Repulsion but no core attraction; (c) No repulsion but core attraction; (d) Repulsion and core attraction.

been around the virtual core, showing the characteristics of mobile formation with the change of potential field. Finally, the task was completed.

There are many classic designs of UAV path planning based on APF method, which aim at single UAV. References [20] and [21] have carried out obstacle avoidance research on multiple UAVs. They regard UAVs as dynamic obstacles, but only introduce repulsion between UAVs, which cannot realize cluster and formation control. The simulation performance is shown in Figure 7b and Figure 9b. In this paper, the core attraction is introduced into the APF method. On the basis of the original function, it can achieve better cluster control effect. The simulation performance is shown in Figure 7d and Figure 9d.

Figure 12 shows the variation trend of distance between the three UAVs and the virtual core during the whole flight.

With the advancement of flight process, the distance between UAV and virtual core will fluctuate slightly due to the influence of obstacles in potential field. This distance has been maintained at about 3m, which shows that the virtual core has a strong binding force on three UAVs, but also reflects a strong formation adaptive ability.

Figure 13 shows the relative position of the three UAVs and the virtual core at eight time points during the flight. According to the corresponding analysis of Figure 12, it is more intuitive to show that the virtual core has strong cluster flight control ability and formation adaptive ability for three UAVs. Figure 14 shows the smooth change trend of the distance from the three UAVs to the target point during the flight.

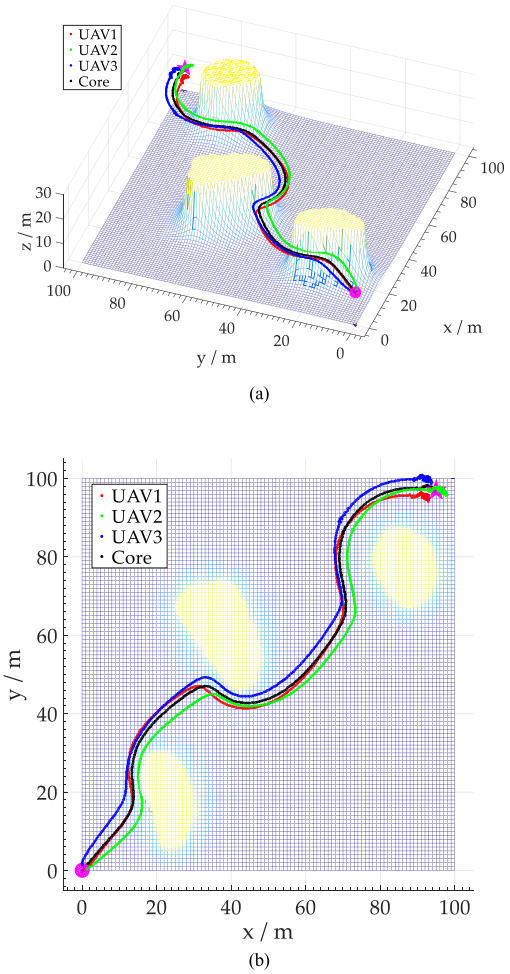

FIGURE 11. 3D and 2D visualization of cluster effect based on virtual core: (a) 3D visualization; (b) 2D visualization.

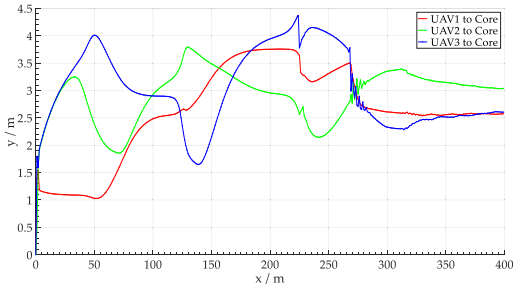

FIGURE 12. Distance from each UAV to the virtual core.

C. CLUSTER RECONFIGURATION PERFORMANCE ANALYSIS

1) SIMULATION SCENE

In the scene of irregular obstacle potential field in Figure 3, taking four UAVs as an example, the cluster reconstruction performance of the algorithm is verified by simulation from the following three aspects: 1) in the process of four UAVs cluster flight execution, when one UAV fails due to external factors, the cluster flight and task execution effect of the remaining three UAVs after the reorganization. 2) in the process of three UAVs cluster flight and mission execution, when the fourth UAVs is ordered to join, the four UAVs cluster

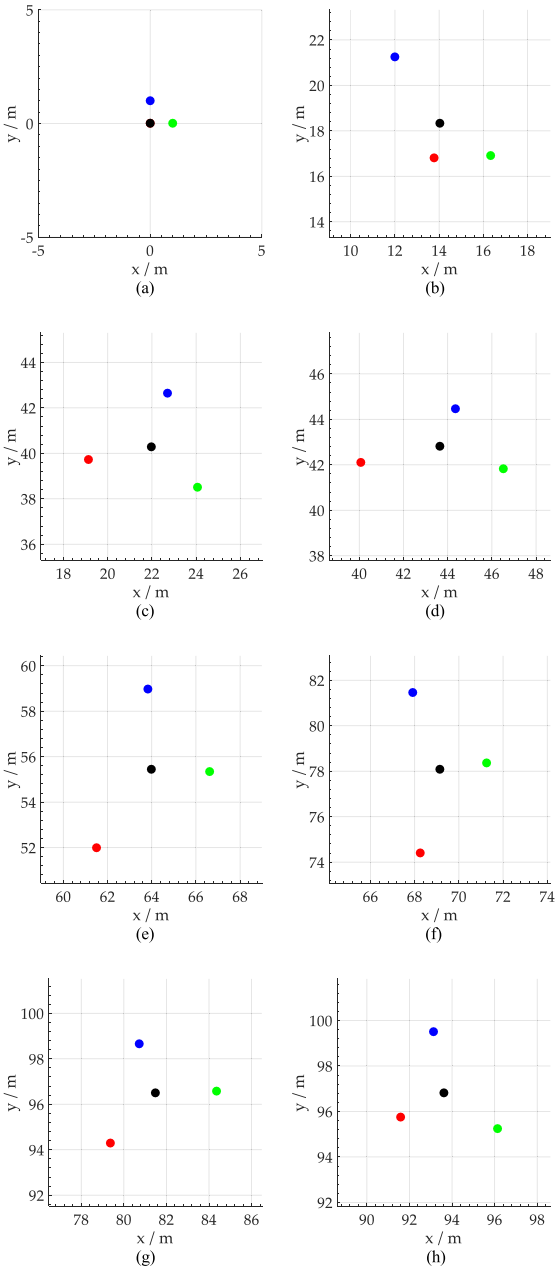

FIGURE 13. Instantaneous position relationship between three UAVs and virtual core: (a) 0s; (b) 50s; (c) 100s; (d) 150s; (e) 200s; (f) 250s; (g) 300s; (h) 400s.

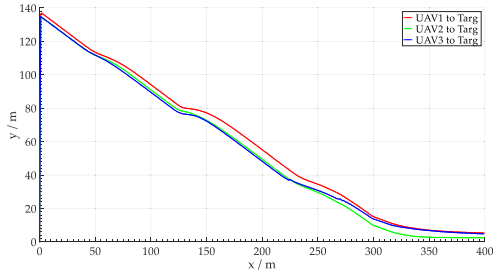

FIGURE 14. Distance from each UAV to the target point.

flight and mission execution effect after reorganization. 3) in the process of four UAVs cluster flight execution, when one or more UAVs are dispatched to perform other tasks, the cluster flight and task execution effect of the remaining UAVs after reorganization.

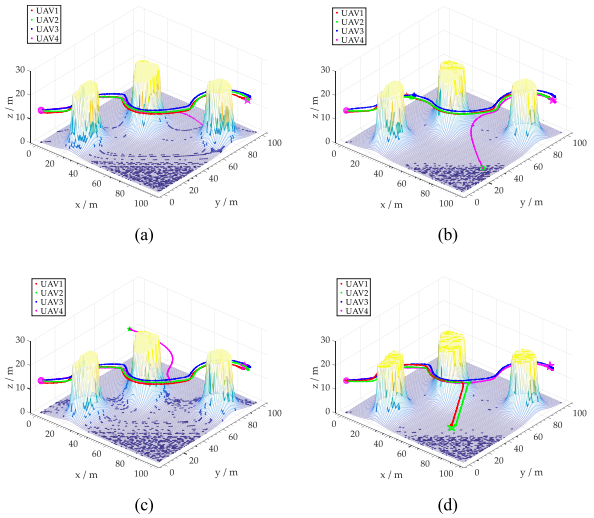

FIGURE 15. Performance of algorithm in UAV cluster reconfiguration: (a) Failure of a UAV; (b) One other drone enters; (c) Dispatch a UAV to (0,90); (d) Dispatch two UAVs to (90,0).

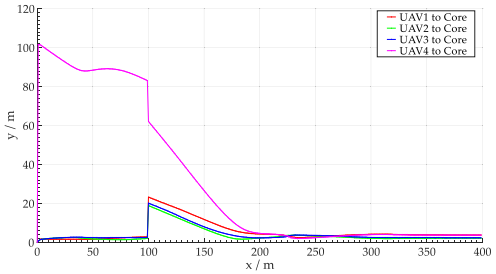

FIGURE 16. Distance from each UAV to the core when the new UAV enters.

2) SIMULATION RESULTS

Figure 15 shows the performance of cluster reconfigure-tion when a UAV fails, merges or schedules in the process of executing cluster tasks. In Figure 15a, an UAV fails in 200s due to external factors. In Figure 15b, when the original cluster flew to 100s, the fourth UAV was instructed to import. In Figure 15c and Figure 15d, the UAV gets the scheduling instruction at 200s and goes to other target points to perform tasks. The simulation results show that when a UAV fails, merges or schedules, the cluster control algorithm has good performance of cluster reconfiguration, which makes the UAV cluster maintain a good flight formation and success-fully reach the target point to complete the task.

In addition, Figure 15b shows that when the cluster flies to 100s, four UAVs receive the new UAV import command at the same time. However, the original three UAVs clusters are not eager to merge with the fourth UAV for reconstruction, but according to the track planning to the target point, choose the right time to reconstruct the cluster, which reflects the good performance of the multi UAV cluster control method based on the virtual core in the improved APF in the track optimization. Figure 16 shows the distance curve from each UAV to the virtual core when the fourth UAV enters.

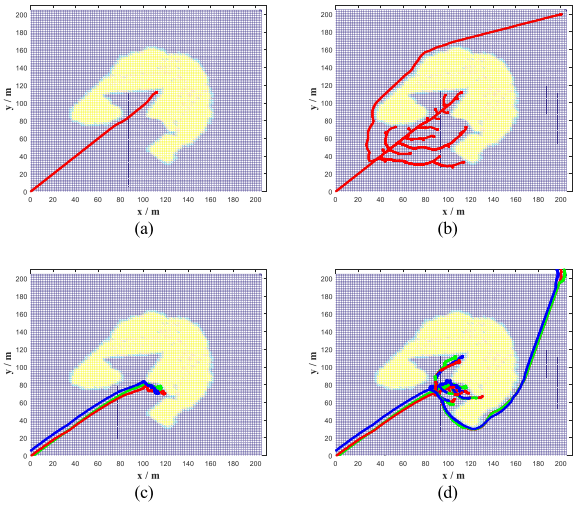

FIGURE 17. Simulation performance of UAV falling into and escaping from local minimum value (a) Single UAV falling into; (b) Single UAV escaping; (c) UAV group falling into; (d) UAV group escaping.

In [23], based on the second-order consensus algorithm and leader follower strategy, the obstacle avoidance problem of UAV group is studied. However, when a UAV in the unit fails, especially the leader failure, it will bring great trouble to the cluster control, and even lead to mission failure. In contrast, the proposed method in this paper has better performance in cluster reconfiguration performance, and the simulation results are shown in Figure 15.

D. BACKTRACKING-FILLING METHOD SIMULATION ANALYSIS

1) SIMULATION SCENE

In the classical APF method, there is a local minimum problem. It is more difficult to solve the local minimum problem caused by dense concave obstacles. In order to verify the applicability of backtracking filling algorithm, a compact concave obstacle is set up in the area of 100m multiplied by 100m, and the APF is established. From the following two aspects, the simulation verifies and compares the effect of backtracking filling method in solving the local minimum problem in APF: 1) single UAV performs tasks. 2) three UAVs cluster to perform tasks.

2) SIMULATION RESULTS

Figure 17 shows the simulation performance of the UAV falling into the local minimum value leading to the mission failure and the UAV escaping from the local minimum value to complete the task in the APF of concave obstacles. In Figure 17a and Figure 17c, the UAV is trapped in the local minimum of the APF without the backtracking-filling algorithm, and the mission fails. In Figure 17b and Figure 17d, backtracking-filling algorithm is used to overcome the local minimum problem. When the UAV reaches the local minimum value of APF, the virtual obstacle is placed, and the UAV returns to a position on the original path, and the distance from the position to the nearest obstacle is greater than R2.

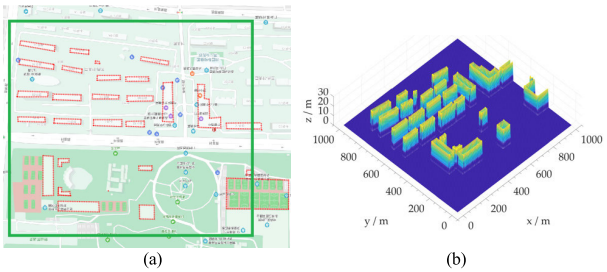

FIGURE 18. Establishment of real scene simulation potential field: (a) Beijing National Olympic Village; (b) Realistic APF.

Then the APF is updated and the path is re planned until the UAV successfully escapes the local minimum value. Each tree-like line from the top to the root in Figure 17b is a process of backtracking and new path. Compared with Figure 17b and Figure 17d, it can be seen that the backtracking-filling method has higher efficiency in path planning when multiple UAVs cluster to perform tasks.

At present, there are a lot of researches on the local minimum caused by coefficient obstacles or compact convex obstacles in APF, but few are focused on compact concave obstacles. In [17], when the UAV group enters a concave obstacle which is represented by two finite walls forming an angle 120 °, the algorithm guides the UAV group to turn right and escape the so-called "stuck state" by inserting an additional control. This method is only discussed and studied for simple concave obstacles. In contrast, the backtracking filling method proposed in this paper can be applied to complex concave obstacles. In addition, when a UAV in the group has filled a local minimum point in the APF, other UAVs will not fall into the local minimum point again, which improves the efficiency of path planning. However, this method has the possibility of further optimization in reducing search time and parameter selection rules.

E. REAL SCENE SIMULATION ANALYSIS

1) SIMULATION SCENE

In practical application, the UAVs may encounter different kinds and density of obstacles. In order to prepare for the real experimentation in the future, this paper takes the National Olympic Village in Beijing as an example, a 1000m times 1000m area is selected to establish an APF, and carries out simulation research. The real area includes residential buildings, hotels, office buildings, monuments, tennis courts, badminton courts, basketball courts, roads, trees, squares and other factors, as shown in Figure 18a. In this paper, without considering the height difference, we select 24 complete buildings as obstacles, set 1m times 1m as the minimum potential grid, and build the APF, as shown in Figure 18b.

2) SIMULATION RESULTS

In the real scene simulation APF, we take three UAVs cluster as an example to carry out simulation verification. The simulation experiment is divided into two groups according to the different target points, one is set as (900,900), the other is set as (400,900). We divide each group of experiments into two

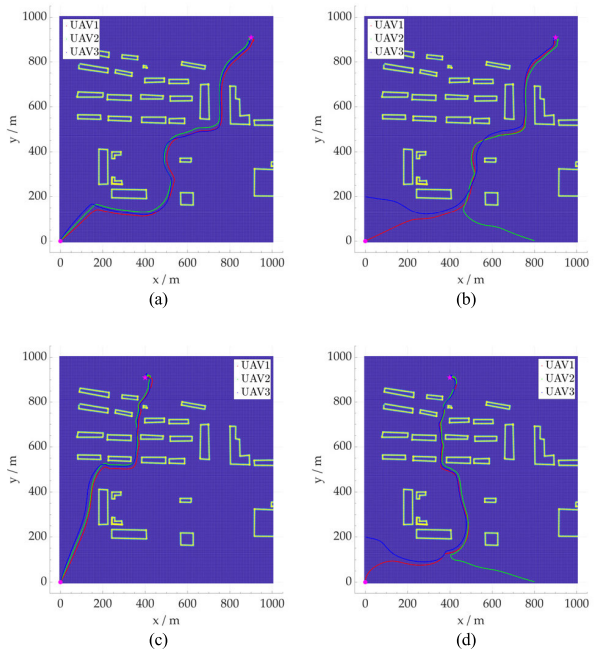

FIGURE 19. 2D visualization of multi UAV mission in urban environme-nt: (a) Same takeoff point to (900,900); (b) Different takeoff point to (900,900); (c) Same takeoff point to (400,900); (d) Different takeoff point to (400,900).

categories according to different takeoff bases, and carry out comparative simulation. One is that three UAVs take off from the same base to perform tasks, the other is that three UAVs take off from three different bases to perform tasks.

Figure 19 shows a 2D visualization of the simulation of multiple UAVs performing tasks in an urban environment under different conditions. Four simulation results show that the UAV successfully reaches the target point and completes the mission after the flight process of mobile formation. Compared with Figure 19c and Figure 19d, it can be seen that the flight priority of the cluster formation is higher than that of the track planning on the premise that the number of individuals in the cluster does not change. The whole flight process shows excellent cluster control effect. The formation shape changes adaptively according to the influence of obstacles. The above simulation results verify the effective-ness of the multi UAV cluster control algorithm based on virtual core.

V. CONCLUSION

This paper presents a virtual core based multi UAV cluster control algorithm in improved APF. We propose the concept of disturbance component and the backtracking-filling method to solve the problem of minimum value of traditional APF. Based on the consideration of potential field repulsion, this paper integrates the attraction of UAV, introduces the concept of virtual core, and constructs the virtual core of multi UAV cluster control. The repulsive force of the artificial potential field can achieve the collision avoidance between the UAVs while avoiding the collision between the UAV and the obstacle and then achieve the purpose of avoiding the obstacle. The virtual core attraction guides multiple UAVs to enter the cluster formation flying, so as to realize the uncertain formation shape of the cluster. This method improves the adaptability of the cluster and reduces the useless energy consumption. The attraction of the target point can make the UAV avoid every local minimum position around the obstacle and continue to move towards the target point by bypassing the obstacle. In addition, this paper proposes a cluster reconfiguration mechanism, which realizes the fault tolerance operation, import and scheduling of UAV in the process of cluster flight, and improves the flexibility and success rate of task execution. In the self-built APF and the simulation potential field based on the urban environment, a variety of simulation experiments are carried out to verify the effectiveness of the algorithm in the multi UAV cluster control. However, the algorithm does not consider the height difference of obstacles, and with the increase of potential field area, it highly depends on the computing performance of the processor. In the future, on the basis of further research, integrating the factors such as obstacle altitude difference and flight altitude, we will carry out the real experimentation of UAV cluster.

REFERENCES

[1] Y. Liu and R. Bucknall, "A survey of formation control and motion planning of multiple unmanned vehicles," *Robotica*, vol. 36, no. 7, pp. 1019–1047, Jul. 2018, doi: 10.1017/S0263574718000218.

[2] J. F. Guerrero-Castellanos, A. Vega-Alonzo, S. Durand, N. Marchand, V. R. Gonzalez-Diaz, J. Castañeda-Camacho, and W. F. Guerrero-Sánchez, "Leader-following consensus and formation control of VTOL-UAVs with event-triggered communications," *Sensors*, vol. 19, no. 24, p. 5498, 2019, doi: 10.3390/s19245498.

[3] X. Peng, K. Guo, and Z. Geng, "Full state tracking and formation control for under-actuated VTOL UAVs," *IEEE Access*, vol. 7, pp. 3755–3766, 2019, doi: 10.1109/ACCESS.2018.2889370.

[4] H. Du, W. Zhu, G. Wen, Z. Duan, and J. Lu, "Distributed formation control of multiple quadrotor aircraft based on nonsmooth consensus algorithms," *IEEE Trans. Cybern.*, vol. 49, no. 1, pp. 342–353, Jan. 2019, doi: 10.1109/TCYB.2017.2777463.

[5] J. Zhang, J. Yan, and P. Zhang, "Fixed-wing UAV formation control design with collision avoidance based on an improved artificial potential field," *IEEE Access*, vol. 6, pp. 78342–78351, 2018, doi: 10.1109/ACCESS.2018.2885003.

[6] S. Monteiro and E. Bicho, "A dynamical systems approach to behavior-based formation control," in *Proc. IEEE Int. Conf. Robot. Automat.*, May 2002, pp. 2606–2611, doi: 10.1109/ROBOT.2002.1013624.

[7] C. Park, N. Cho, K. Lee, and Y. Kim, "Formation flight of multiple UAVs via onboard sensor information sharing," *Sensors*, vol. 15, no. 7, pp. 17397–17419, Jul. 2015, doi: 10.3390/s150717397.

[8] Á. Madridano, A. Al-Kaff, D. Martín and A. de la Escalera, "3D trajectory planning method for UAVs swarm in building emergencies," *Sensors*, vol. 20, no. 3, p. 642, 2020, doi: 10.3390/s20030642.

[9] Y.-B. Chen, G.-C. Luo, Y.-S. Mei, J.-Q. Yu, and X.-L. Su, "UAV path planning using artificial potential field method updated by optimal control theory," *Int. J. Syst. Sci.*, vol. 47, no. 6, pp. 1407–1420, 2016, doi: 10.1080/00207721.2014.929191.

[10] T. Y. Abdalla, A. A. Abed, and A. A. Ahmed, "Mobile robot navigation using PSO-optimized fuzzy artificial potential field with fuzzy control," *J. Intell. Fuzzy Syst.*, vol. 32, no. 6, pp. 3893–3908, May 2017, doi: 10.3233/IFS-162205.

[11] A. Melingui, R. Merzouki, J. B. Mbede, and T. Chettibi, "A novel approach to integrate artificial potential field and fuzzy logic into a common framework for robots autonomous navigation," *Proc. Inst. Mech. Eng., I, J. Syst. Control Eng.*, vol. 228, no. 10, pp. 787–801, Nov. 2014, doi: 10.1177/0959651814548300.

[12] Z. Zhou, J. Wang, Z. Zhu, D. Yang, and J. Wu, "Tangent navigated robot path planning strategy using particle swarm optimized artificial potential field," *Optik*, vol. 158, pp. 639–651, Apr. 2018, doi: 10.1016/j.ijleo.2017.12.169.

[13] H. Min, Y. Lin, S. Wang, F. Wu, and X. Shen, "Path planning of mobile robot by mixing experience with modified artificial potential field method," *Adv. Mech. Eng.*, vol. 7, no. 12, pp. 1–17, 2015, doi: 10.1177/1687814015619276.

[14] R. A. Sasongko, S. S. Rawikara, and H. J. Tampubolon, "UAV obstacle avoidance algorithm based on ellipsoid geometry," *J. Intell. Robot. Syst.*, vol. 88, nos. 2–4, pp. 567–581, Dec. 2017, doi: 10.1007/s10846-017-0543-4.

[15] Q. Wu, X. Shen, Y. Jin, Z. Chen, S. Li, A. H. Khan, and D. Chen, "Intelligent beetle antennae search for UAV sensing and avoidance of obstacles," *Sensors*, vol. 19, no. 8, p. 1758, Apr. 2019, doi: 10.3390/s19081758.

[16] P. Fraga-Lamas, L. Ramos, V. Mondéjar-Guerra, and T. M. Fernández-Caramés, "A review on IoT deep learning UAV systems for autonomous obstacle detection and collision avoidance," *Remote Sens.*, vol. 11, no. 18, p. 2144, Sep. 2019, doi: 10.3390/rs11182144.

[17] S. Iovino, A. R. Vetrella, G. Fasano, D. Accardo, and A. Savvaris, "Implementation of a distributed flocking algorithm with obstacle avoidance capability for UAV swarming," in *Proc. AIAA Inf. Syst.-AIAA Infotech @ Aerosp.*, Jan. 2017, p. 0878, doi: 10.2514/6.2017-0878.

[18] Z. Pan, D. Li, K. Yang, and H. Deng, "Multi-robot obstacle avoidance based on the improved artificial potential field and PID adaptive tracking control algorithm," *Robotica*, vol. 37, no. 11, pp. 1883–1903, Nov. 2019, doi: 10.1017/S026357471900033X.

[19] D. Wang, P. Wang, X. Zhang, X. Guo, Y. Shu, and X. Tian, "An obstacle avoidance strategy for the wave glider based on the improved artificial potential field and collision prediction model," *Ocean Eng.*, vol. 206, Jun. 2020, Art. no. 107356, doi: 10.1016/j.oceaneng.2020.107356.

[20] X. Wang, Y. Liang, S. Liu, and L. Xu, "Bearing-only obstacle avoidance based on unknown input observer and angle-dependent artificial potential field," *Sensors*, vol. 19, no. 1, p. 31, Dec. 2018, doi: 10.3390/s19010031.

[21] J. Tang, J. Sun, C. Lu, and S. Lao, "Optimized artificial potential field algorithm to multi-unmanned aerial vehicle coordinated trajectory planning and collision avoidance in three-dimensional environment," *Proc. Inst. Mech. Eng., G, J. Aerosp. Eng.*, vol. 233, no. 16, pp. 6032–6043, Dec. 2019, doi: 10.1177/0954410019844434.

[22] J. Sun, J. Tang, and S. Lao, "Collision avoidance for cooperative UAVs with optimized artificial potential field algorithm," *IEEE Access*, vol. 5, pp. 18382–18390, 2017, doi: 10.1109/ACCESS.2017.2746752.

[23] Y. Du, X. Zhang, and Z. Nie, "A real-time collision avoidance strategy in dynamic airspace based on dynamic artificial potential field algorithm," *IEEE Access*, vol. 7, pp. 169469–169479, 2019, doi: 10.1109/ACCESS.2019.2953946.

[24] Y. Huang, J. Tang, and S. Lao, "UAV group formation collision avoidance method based on second-order consensus algorithm and improved artificial potential field," *Symmetry*, vol. 11, no. 9, p. 1162, Sep. 2019, doi: 10.3390/sym11091162.

[25] Y. Zhang, W. Feng, G. Shi, F. Jiang, M. Chowdhury, and S. H. Ling, "UAV swarm mission planning in dynamic environment using consensus-based bundle algorithm," *Sensors*, vol. 20, no. 8, p. 2307, Apr. 2020, doi: 10.3390/s20082307.

[26] J. Ghommam, H. Mehrjerdi, M. Saad, and F. Mnif, "Formation path following control of unicycle-type mobile robots," *Robot. Auton. Syst.*, vol. 58, no. 5, pp. 727–736, May 2010, doi: 10.1016/j.robot.2009.10.007.

[27] H. Mehrjerdi, J. Ghomman, and M. Saan, "Nonlinear coordination control for a group of mobile robots using a virtual structure," *Mechatronics*, vol. 21, no. 7, pp. 1147–1155, Oct. 2011, doi: 10.1016/j.mechatronics.2011.06.006.

[28] X. Xiao, Z. Dong, J. Wu, and H. Duan, "A cooperative approach to multiple UAVs searching for moving targets based on a hybrid of virtual force and receding horizon," in *Proc. 10th Int. Conf. Ind. Inform.*, 2012, pp. 1228–1233.

[29] B. Shirani, M. Najafi, and I. Izadi, "Cooperative load transportation using multiple UAVs," *Aerosp. Sci. Technol.*, vol. 84, pp. 158–169, Jan. 2019, doi: 10.1016/j.ast.2018.10.027.

[30] F. A. A. Andrade, A. Hovenburg, L. N. D. de Lima, C. D. Rodin, T. A. Johansen, R. Storvold, C. A. M. Correia, and D. B. Haddad, "Autonomous unmanned aerial vehicles in search and rescue missions using real-time cooperative model predictive control," *Sensors*, vol. 19, no. 19, p. 4067, Sep. 2019, doi: 10.3390/s19194067.

[31] Z. Zhen, Y. Chen, L. Wen, and B. Han, "An intelligent cooperative mission planning scheme of UAV swarm in uncertain dynamic environment," *Aerosp. Sci. Technol.*, vol. 100, May 2020, Art. no. 105826, doi: 10.1016/j.ast.2020.105826.

[32] X. D. Z. Z. Huajun, "Cooperative search of UAV swarm based on ant colony optimization with artificial potential field," *Trans. Nanjing Univ. Aeronaut. Astronaut.*, vol. 36, no. 6, pp. 912–918, 2019, doi: 10.16356/j.1005-1120.2019.06.004.

[33] M. Mavrovouniotis, C. Li, and S. Yang, "A survey of swarm intelligence for dynamic optimization: Algorithms and applications," *Swarm Evol. Comput.*, vol. 33, pp. 1–17, Apr. 2017, doi: 10.1016/j.swevo.2016.12.005.

ENMING WU was born in Shandong, China, in 1985. He received the master's degree in detection technology and automation equipment from the Tianjin University of Science and Technology, in 2011. He is currently the Director of electronic technology innovation and entrepreneurship practice base of the Civil Aviation University of China. His main research interests include UAV formation flight control and artificial intelligence control.

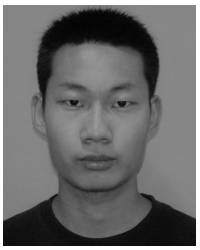

YIDONG SUN was born in Dalian, China. He received the bachelor's degree in electrical engineering and automation from the Civil Aviation University of China, in 2019. His main research interests include UAV cluster control, UAV application, robotics, and artificial intelligence.

JIANYU HUANG was born in Henan, China, in 1969. He received the master's degree in communication and electronic system from the Nanjing University of Aeronautics and Astronautics, in 1996, and the Ph.D. degree in signal and information processing from Tianjin University, in 2007. He is currently the Director and an Associate Professor with the Electrical and Electronic Experiment Center, Civil Aviation University of China. His main research interests include image processing and digital signal processing.

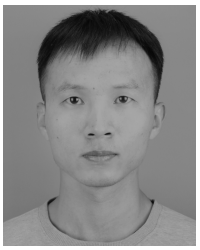

CHAO ZHANG was born in Hebei, China. He received the master's degree in electrical engineering from the Harbin University of Technology, in 2016. His main research interests include UAV control and artificial intelligence algorithm.

ZHIHENG LI was born in Hainan, China. He is currently pursuing the degree in aircraft manufacturing engineering with the Civil Aviation University of China. His main research interests include UAV control algorithm and UAV formation control.